Diffusion Behavior of Lipid Vesicles in Entangled Polymer Solutions

Xingxiang Cao,* Rama Bansil,# Donald Gantz,§ Edward W. Moore,¶ Niu Niu,‖ and Nezam H. Afdhal‖
Departments of *Chemistry and #Physics, Boston University, Boston, Massachusetts 02215; §Department of Biophysics, Boston University School of Medicine, Boston, Massachusetts 02118; ¶Medical College of Virginia, Richmond, Virginia 23298; and ‖Section of Gastroenterology, Evans Department of Medicine and Thorndike Memorial Laboratories, Boston City Hospital, Boston, Massachusetts 02118 USA

ABSTRACT Dynamic light scattering was used to follow the tracer diffusion of phospholipid/cholesterol vesicles in aqueous polyacrylamide solutions and compared with the diffusive behavior of polystyrene (PS) latex spheres of comparable diameters. Over the range of the matrix concentration examined (C_p = 0.1–10 mg/ml), the diffusivities of the PS spheres and the large multilamellar vesicles exhibited the Stokes-Einstein (SE) relation, while the diffusivity of the unilamellar vesicles did not follow the increase of the solution's viscosity caused by the presence of the matrix molecules. The difference between the diffusion behaviors of unilamellar vesicles and hard PS spheres of similar size is possibly due to the flexibility of the lipid bilayer of the vesicles. The unilamellar vesicles are capable of changing their shape to move through the entangled polymer solution so that the hindrance to their diffusion due to the presence of the polymer chains is reduced, while the rigid PS spheres have little flexibility and they encounter greater resistance. The multilamellar vesicles are less flexible, thus their diffusion is similar to the hard PS spheres of similar diameter.

INTRODUCTION

In recent years there has been a growing interest in the study of liquid dispersions consisting of particles, macromolecules, and solvent, both because of their technological importance (National Research Council, 1988) and the fundamental properties of complex fluids. Examples of these so-called composite liquids include ceramic precursors, lubricants, paints, adhesives, and the cytoplasm in biological cells. The rheological behavior and dynamics of such complex fluids have many interesting and unusual features and have been extensively investigated. Tracer diffusion studies using dynamic light scattering (DLS) of spherical probe particles have been employed to study the properties of the polymer solutions and gels in which the particles are incorporated (Brown and Rymden, 1988; Brown and Zhou, 1989, 1990; Cooper et al., 1991; Lin and Phillies, 1984; Nehme et al., 1989; Onyenemezu et al., 1993; Phillies, 1990; Phillies et al., 1987; Reina et al., 1990; Tracy and Pecora, 1992; Won et al., 1994). In biological systems, tracer diffusion has been used to determine state of aggregation and effective viscosity of the macromolecular solution (Madonia et al., 1983; Newman and Schick, 1989; Newman et al., 1989; San Biagio et al., 1991). The diffusivity of a sphere is typically discussed via the Stokes-Einstein (SE) relation:

$$D = \frac{k_B T}{6\pi\eta R} \quad (1)$$

where k_B is the Boltzmann's constant, T is the temperature, R is the hydrodynamic radius of the sphere, and η is the viscosity of the medium in which the sphere is suspended. The SE relation works perfectly for non-interacting spheres in a small-molecule solvent. If the size of the spheres remains constant, then $D/D_0 = \eta_0/\eta$, i.e., $D\eta/(D_0\eta_0) = 1$, where D_0 is the infinite dilution diffusivity of the spheres and η_0 is the solvent viscosity. However, it is certainly not obvious that an arbitrary polymer solution will satisfy the continuum assumption. Consequently, the deviation of $D\eta/(D_0\eta_0)$ from unity implies that either the viscosity felt by the probe particle is different from the bulk viscosity, or that the size of the probe particle has changed. Both positive deviation, $D\eta/(D_0\eta_0) > 1$, and negative deviation, $D\eta/(D_0\eta_0) < 1$, have been observed (Won et al., 1994). One may use the measured diffusivity of a sphere of constant size R to define a "microviscosity" or "effective viscosity" of the solution using the SE relation. A positive deviation from SE behavior therefore corresponds to a microviscosity less than the macroscopic viscosity of the solution, whereas a negative deviation is indicative of either particle aggregation, or polymer adsorption on the particle, or polymer/particle interactions leading to an increased viscosity in the solution.

Two aspects of tracer diffusion of spherical particles in polymer solutions have been emphasized in previous studies. The first deals with the question of how the concentration of the polymer solution affects the diffusion of the spherical probe particle, and the second deals with the question of how the architecture of the polymer matrix, i.e., linear, branched, or gel, affects the diffusion of the spherical probe particle. Our focus for this particular study has been to compare the diffusion behaviors between two different types of spheres, namely, the solid polystyrene latex particles (PS spheres) and lipid vesicles, which consist of a lipid bilayer with solvent (water) inside. Our goal is to examine whether the different architectures of the tracer particles lead to different diffusion behaviors in identical environments.

Received for publication 15 November 1996 and in final form 23 June 1997.

Address reprint requests to Dr. Rama Bansil, Center for Polymer Studies, Dept. of Physics, Boston University, 590 Commonwealth Ave., Boston, MA 02215. Tel.: 617-353-2969; Fax: 617-353-9393; E-mail: rb@buphy.bu.edu.

0006-3495/97/10/1932/08 $2.00

Understanding the diffusion of vesicles in complex macromolecular matrices is of obvious biological importance. One specific problem, where the interaction of lipid vesicles with proteins has been shown to be of biological significance, is in the formation of cholesterol gallstones in the gallbladder. These protein-lipid interactions are seen with macromolecules such as gallbladder mucin, which has been shown to accelerate both vesicle fusion (Afdhal et al., 1995) and nucleation of cholesterol monohydrate crystals in a time- and concentration-dependent fashion (Smith, 1987). In our previous studies we observed a change in the diffusivity of the vesicles upon the addition of mucin (Afdhal et al., 1995). The question arises as to what causes this change in diffusivity. Is it related to a change in the size of the vesicle due to fusion/aggregation or vesicle-mucin association, or is it simply caused by the change in the viscosity of the solution due to the added polymer? Since mucin is a complicated biopolymer that has a tendency to *associate*, it is important to know how the viscosity of a *non-associating* polymer influences the diffusion of vesicles. With this goal in mind, we investigated the diffusion of vesicles in aqueous solutions of polyacrylamide (PA), which does not have any tendency to associate in the dilute to semi-dilute concentration regime, using the technique of DLS.

MATERIALS AND METHODS

Samples

Polystyrene (PS) latex spheres of different diameters (64 nm and 107 nm) were purchased from Polyscience, Inc., Warrington, PA. The sphere diameters given by the manufacturer were verified by transmission electron microscopy (TEM) and DLS. Water-soluble polyacrylamide (PA) of two different molecular weights ($M_w = 6.5 \times 10^4$, $M_W/M_N = 1.3$; and $M_W = 1.0 \times 10^6$, $M_W/M_N = 3.0$) was also purchased from Polyscience, Inc. Cholesterol, phosphatidylcholine [egg yolk, type V PC in chloroform-methanol, 9:1 (vol/vol)], and sodium taurocholate (NaTC) were obtained from Sigma Chemical Company, St. Louis, MO.

Model bile

Cholesterol supersaturated model bile (CSI 1.4, total lipid 10 g/dl) was prepared by co-precipitation of the lipids from organic solvents as previously described (Smith, 1987). Cholesterol was purified by double recrystallization from hot 95% ethanol, and sodium taurocholate was recrystallized twice by the method of Pope (Pope, 1967). Egg yolk phosphatidylcholine was used as supplied in chloroform-methanol, 9:1 (vol/vol). Model bile was labeled by adding 1 μl (@ 80,000 DPM) of ^{14}C-cholesterol and ^{3}H-PC (New England Nuclear, Boston, MA). The total lipid concentration of model bile was varied from 3 g/dl to 10 g/dl with a molar ratio of phosphatidylcholine/(NaTC + phosphatidylcholine) of 0.2. After co-precipitation of lipids in a rotary evaporator, model biles were suspended in 0.01 mol/l Tris-HCl, pH 7.0 buffer containing 0.145 mol/l NaCl, heated at 80°C for 1 h to achieve an isotropic phase, and then filtered through a sterile 0.22 μm filter. Model biles were equilibrated at 37°C for 4 h before vesicle separation by chromatography.

Small unilamellar vesicle preparation

Small unilamellar vesicles (65 nm in diameter by DLS and TEM) were prepared by gel filtration chromatography. Model bile (0.5 ml) was applied to a Pharmacia fast protein liquid chromatography (FPLC) system equipped with a Superose 6 gel filtration column equilibrated with 7.5 mol/l NaTC solution at 1 ml/min (Cohen and Carey, 1990). Separation of bile into vesicular and micellar fractions was confirmed by radiochemical assay of column fractions in an LKB 12-14 liquid scintillation counter and measuring cholesterol (Rudell and Morris, 1973), bile salts (Turley and Dietschy, 1978), and phospholipid (Bartlett, 1959). Vesicular cholesterol to phospholipid ratio in the vesicles was 1.6:1.

Large extrusion vesicle preparation

Large vesicles were produced by the extrusion technique (MacDonald et al., 1991). Cholesterol and phosphatidylcholine were co-precipitated and mixed to obtain the isotropic phase, as described in the Model Bile section, and then freeze-thawed 10 times to ensure solute equilibration between trapped and bulk solutions (MacDonald et al., 1983; Mayer et al., 1985). The multilamellar vesicles were extruded through a polycarbonate membrane filter (membrane pore diameter: 100 nm) mounted in the mini-extruder (LiposoFast-Basic, Avestin, Inc., Ottawa, Canada) to generate large vesicles of a uniform 100-nm size. The total lipid concentration was varied from 1 g/dl to 6 g/dl with different molar ratios of cholesterol/phosphatidylcholine ranging from 0 to 1.3. A complex of 50% unilamellar and 50% multilamellar vesicles, 105 nm in diameter by DLS, was prepared by the extrusion technique.

Transmission electron microscopy

Transmission electron microscopy (TEM) studies were initially performed to confirm that both FPLC and extrusion techniques resulted in acceptable preparation of vesicles, which could then be used in the diffusion studies described below.

Lipid vesicles were examined by negative stain TEM using previously published techniques (Afdhal et al., 1995; Somjen et al., 1986; Forte and Nordhausen, 1986). PS spheres were examined by placing a 7-μl undiluted sample on a glow-discharged carbon, formvar-coated 300 mesh copper grid, incubating for 15 to 60 s, blotting, and air drying. Images were recorded on SO-163 film in a Philips CM-12 transmission electron microscope at a magnification of 22,000.

To investigate lamellar structure, both FPLC and extrusion vesicles were further studied using vitreous ice cryomicroscopy (Dubochet et al., 1988). Just before freezing, vesicle samples were diluted at least 1:5 with pure water (to a concentration of 6 mg/ml) in order to reduce concentration of NaCl in buffer and promote rapid freezing. An 8-μl aliquot of each sample was placed on a freshly glow-discharged holey carbon, formvar film on a 400 mesh grid held by hanging forceps in a humidity chamber, blotted from the underside with filter paper, and immediately plunged into an ethane slurry cooled with liquid nitrogen. Vitrified samples were transferred to a Gatan Single Tilt Cryoholder (Model 613) in a Gatan Cryotransfer Station (Model 626). Samples were maintained at −172°C while images were recorded on SO-163 film under low dose conditions in a Philips CM-12 transmission electron microscope.

Viscosity measurements

The polymer solution viscosity was measured using a Cannon Ubbelohde semi-micro viscometer at room temperature. The measured viscosity values were normalized by using the viscosity of water at room temperature as a standard. The results are shown in Fig. 1 for PA aqueous solutions of two different molecular weights, $M_w = 6.5 \times 10^4$ and $M_w = 1.0 \times 10^6$, respectively.

Dynamic light scattering

DLS measurements were performed with a Brookhaven Instruments Corporation (BIC) BI-9000 correlator using the $\lambda = 514.5$ nm line of an Argon

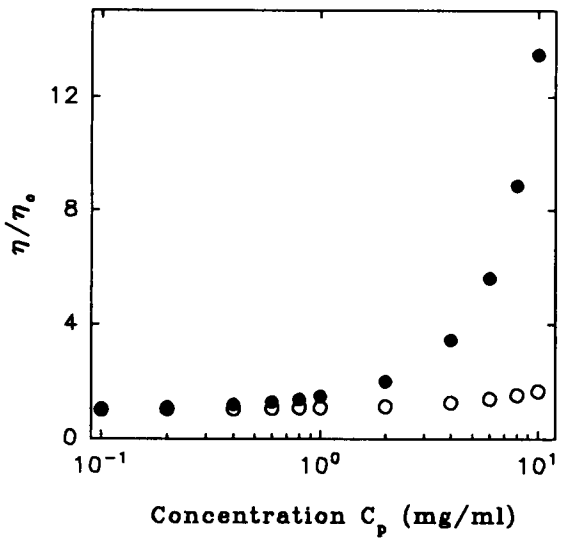

FIGURE 1 Viscosity versus concentration of polyacrylamide solution. η is polymer solution viscosity, η_0 is the viscosity of water (solvent) at room temperature. ○, $M_W = 6.5 \times 10^4$; ●, $M_W = 1.0 \times 10^6$.

laser to illuminate the sample and a BIC goniometer. The scattered intensity at scattering angle θ was detected using standard photon counting methods. Intensity autocorrelation functions, $G_2(t)$, covering the decay of the intensity fluctuations over six decades of time were measured.

The decay of the intensity autocorrelation function, $G_2(t)$, provides a measure of the diffusion coefficient of the macromolecules in the solution (Berne and Pecora, 1976). If there is only one size of the macromolecule in dilute solution, then

$$G_2(t) = B + A \exp(-2Dq^2t) \quad (2)$$

where A denotes the dynamic amplitude and D the diffusion coefficient of the macromolecule. B denotes the baseline of the measured correlation function (related to the total intensity scattered at the scattering vector $q = (4\pi n/\lambda)\sin(\theta/2)$, where n is the refractive index of the solvent). In a polydisperse solution, there may be many different species each diffusing with its own characteristic diffusion coefficient. In this case it is possible to obtain the distribution $A(D)$ of species with diffusion coefficient D from the normalized electric field autocorrelation function, $g_1(t) = [(G_2(t) - B)/A]^{1/2}$ by writing $g_1(t) = \int A(D) \exp(-Dq^2t)\, dD$. The distribution function can be determined by Laplace inversion techniques.

The intensity correlation functions were measured over scattering angles of 30–130° at a temperature 25.0 ± 0.1°C. The resulting distribution of diffusion coefficients $A(D)$ was obtained by Laplace inversion using the CONTIN program (Provencher et al., 1978).

Vesicles were mixed into polymer solution to achieve the polymer concentration desired, equilibrated overnight, and DLS measurements were performed the following day. Similar procedure was used for the PS spheres in polymer solutions. Vesicle + PA solutions, monitored by DLS right after mixing, were found to be stable for longer than 24 h, indicating that the integrity of the vesicles is maintained.

RESULTS AND DISCUSSION

TEM images of FPLC and extrusion vesicles in ice are shown in Fig. 2, *A* and *B*, respectively. FPLC vesicles were spherical, 97% unilamellar, highly monodisperse with an average diameter of 60 nm, 94% of FPLC vesicles were within the range of 37–72 nm, 6% were 77–237 nm. Extrusion vesicles were more polydisperse, polymorphic, and

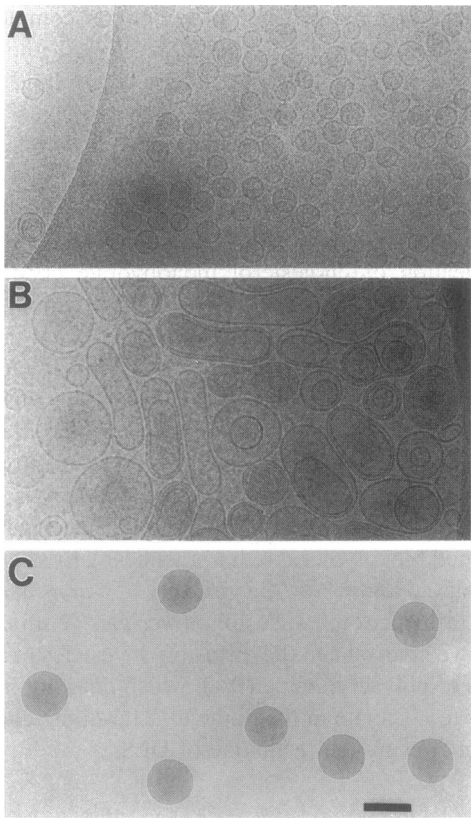

FIGURE 2 Transmission electron micrographs of phospholipid/cholesterol vesicles and polystyrene latex microspheres. Bar = 100 nm. See Material and Methods for preparative techniques. (*A*) FPLC vesicles are shown in vitreous ice in hole at left and in ice over carbon at right. Vesicles are spherical, homogeneous in size, and unilamellar. (*B*) Extrusion vesicles in ice show polymorphism, size heterogeneity, and a 1:1 ratio of unilamellar and multilamellar structure. (*C*) Latex spheres (d = 107 nm) do not show any aggregation in an aqueous solution of polyacrylamide (M_w = 1.0×10^6) at C_P = 1.0 mg/ml.

contained unilamellar and multilamellar structures (1:1). Size quantitation of extrusion vesicles in ice yielded an average diameter of 114 nm, with the population evenly distributed in the range of 34–197 nm. This average diameter by TEM was slightly larger than the 105 nm determined by DLS. This difference was caused by the largest vesicles in the population being squeezed/flattened in the ice layer as observed when comparing images of 0 and 45 tilt. TEM images of PS spheres + polymer solutions do not suggest significant aggregation or adsorption (Fig. 2 *C*).

The angular dependence of the scattered intensity for the 64-nm PS spheres + polymer ($M_w = 1.0 \times 10^6$) solutions with different matrix concentrations is shown in Fig. 3. There is considerable noise in the static scattering data, making quantitative predictions of particle size less reliable than DLS. Within the accuracy of the data no systematic deviations could be observed for solutions of different PA concentrations. For the sample without any added polymer we obtained $d = 56 \pm 5$ nm by fitting the data to the particle scattering form factor for uniform spheres. This calculated diameter of the PS spheres is within the size range $d = 64 \pm$

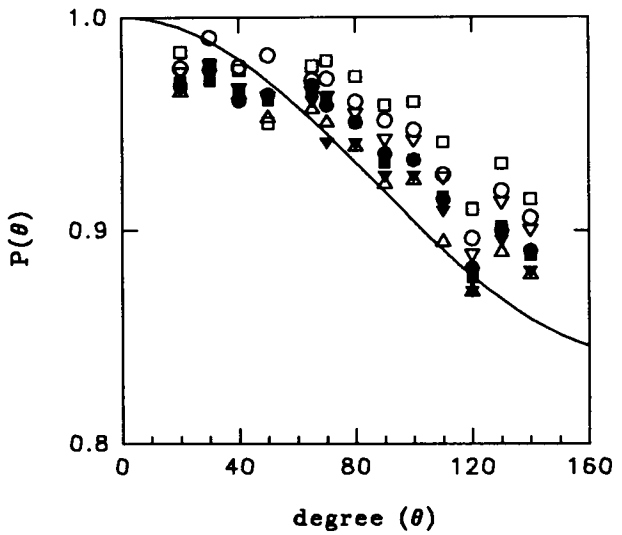

FIGURE 3 Angular dependence of the static scattering intensity for PS spheres (d = 64 nm) in polyacrylamide solutions (M_w = 1.0 × 10^6) at different matrix concentrations in mg/ml. ○, 8.0; ●, 4.0; ▽, 2.0; ▼, 1.0; □, 0.5; ■, 0.1; △, 0.0. The solid line represents the normalized scattering function $P(\theta)$ for a uniform sphere:

$$P(\theta) = \{3[\sin(u) - u\cos(u)]/u^3\}^2,$$

$$u = qa = (4\pi na/\lambda)\sin(\theta/2),$$

where a = 28 nm is the radius of the sphere. This value is obtained by fitting the data for the sample without any added polymer to the scattering form factor for uniform spheres.

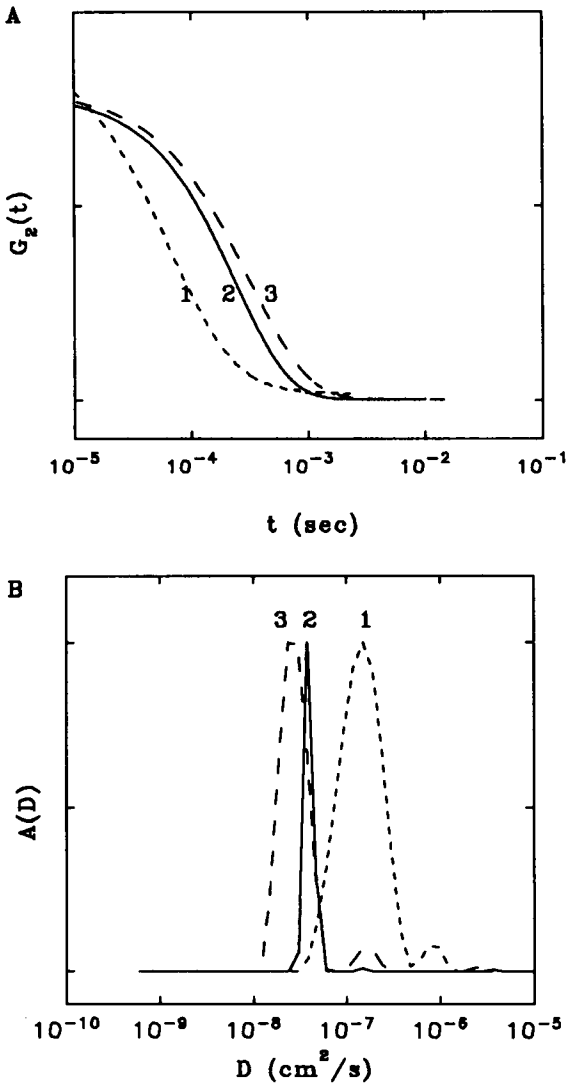

FIGURE 4 (*A*) Intensity correlation functions for vesicle suspensions and polyacrylamide solution measured by DLS at a scattering angle of 90°. (1) Polyacrylamide solution (M_W = 1.0 × 10^6, C_p = 4.0 mg/ml). (2) Large extrusion cholesterol-phospholipid vesicles (d = 105 nm) in aqueous solution. (3) Large extrusion cholesterol-phospholipid vesicles in polyacrylamide solution (M_W = 1.0 × 10^6, C_p = 1.0 mg/ml). (*B*) Distribution of diffusion coefficient $A(D)$ obtained by the CONTIN analysis from the correlation functions shown above.

10 nm given by the manufacturer. The data in general follow the shape of scattering form factor for uniform spheres. The deviation from the uniform sphere form factor is partly caused by the contribution from the random coil PA macromolecules whose form factor decays faster at small angles and slower at large angles than the form factor for uniform spheres. This suggests that the scattering from the particles dominates over the scattering from the polymer solution.

Fig. 4 shows typical intensity autocorrelation functions (Fig. 4 *A*) and the corresponding distribution $A(D)$ obtained by the CONTIN analysis (Fig. 4 *B*) from 1) vesicle-free PA solution, 2) large extrusion vesicle, and 3) large extrusion vesicle in PA solution. As seen in Fig. 4 *B* the $A(D)$ distribution of the pure vesicle suspension shows only one narrow peak centered around 4.5 × 10^{-8} cm^2/s, implying that the vesicles are fairly uniform in size. The $A(D)$ of the vesicle with the polymer added shows a dominant peak which we attribute to the vesicle diffusion in the mixture, and a much weaker peak at higher D values, which has the same D value as the PA's self-diffusion mode; thus we attribute this peak to the diffusion of the PA polymer. This is confirmed by comparing with the $A(D)$ obtained for a pure PA solution that shows a broad peak (the self-diffusion mode) centered around 2 × 10^{-7} cm^2/s. (The much weaker peak at $D \sim 10^{-6}$ cm^2/s is the collective diffusion mode of the PA polymer.) The breadth of the peak reflects the polydispersity in this PA solution. It is important to recognize that the scattering from the PA solution is very weak compared to the vesicles ($I_{s\ (PA)} \leq 20\%\ I_{s\ (vesicle)}$); in order to measure the intensity autocorrelation functions from the pure polymer the incident laser power was doubled and we needed to average the signal for much longer. Therefore, for particle + polymer suspensions, the D values taken from the dominant peak can be regarded as D values for vesicles or PS spheres. At high polymer concentrations, however, the scattering from the unilamellar FPLC vesicles is no longer the dominant source since the scattering from polymer starts to interfere. The CONTIN results become less reliable. Consequently, only the results at concentrations $C_P \leq 4.0$ mg/ml at which the vesicles scatter dominantly are pre-

sented for the unilamellar vesicle + polymer aqueous suspensions.

To confirm that the motion of particles in the polymer solutions is purely diffusive we examined the q-dependence of the DLS measurement. Fig. 5 shows the q-dependence of the decay rate Γ for PS spheres (d = 107 nm) in aqueous solution with and without added polymer. The excellent linear relationship between Γ and q^2 implies that the motion is purely diffusive. The average diffusion coefficient for PS spheres in aqueous solution, $D_{avg} = 4.5 \times 10^{-8}$ cm^2/s obtained from the slope of Γ vs. q^2, is close to that obtained at $\theta = 90°$. The corresponding hydrodynamic diameter, d = 108 nm, compares well with the manufacturer's value. The intercepts at $q = 0$ for all three systems are very close to zero (0 ± 10 s^{-1}), indicating that the particle motion seen by DLS is purely translational diffusion. Subsequently, only DLS measurements made at $\theta = 90°$ are presented.

When the diffusion data from DLS were analyzed as a function of matrix concentration, the change of diffusion coefficient versus matrix concentration could be well described by the "stretched exponential" scaling relation (Phillies, 1988, 1989; Phillies and Peczak, 1988)

$$D = D_0 \exp(-\alpha c^{\mu}) \quad (3)$$

For the large extrusion vesicles in PA solutions (M_W = 1.0×10^6), $\alpha = 0.406$ and $\mu = 0.892$. The $c^{0.892}$ dependence is comparable to that found from other experiments using flexible coils as the matrix polymer (Brown and Rymden, 1988; Phillies, 1989, 1990; Tracey and Pecora, 1992; Zhou and Brown, 1989).

Fig. 6 shows the concentration dependence of D/D_0 for unilamellar FPLC vesicles and PS spheres (d = 64 nm) in low and high molecular weight PA solutions. The inverse of the normalized viscosity, η_0/η, is also shown in this figure. It clearly demonstrates that the concentration dependence of diffusion coefficient is different for unilamellar vesicles as compared to PS spheres, even though both particles are of the same size (d = 65 nm for the vesicles and d = 64 nm for the PS spheres) and are diffusing in identical environments. This difference in diffusion behaviors of unilamellar vesicles versus PS spheres 1) increases with increasing polymer concentration and 2) is larger for the higher molecular weight matrix polymer. We also note that D/D_0 does not coincide with η_0/η, except at low PA concentration.

To further discuss this deviation we re-plot the data shown in Fig. 6 as the ratio $D\eta/(D_0\eta_0)$ versus the polymer concentration C_p for different particle-polymer solutions. In addition to the results for small 64-nm diameter PS spheres

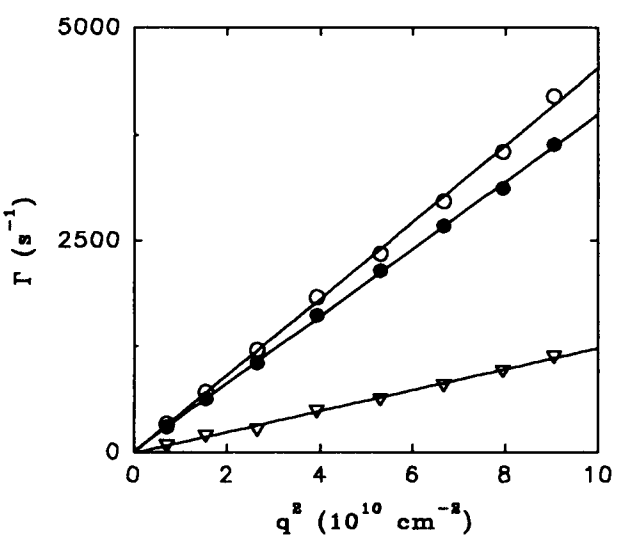

FIGURE 5 The q-dependence of the decay rate, Γ, obtained by the CONTIN analysis for PS spheres (d = 107 nm) in aqueous solutions with and without added polyacrylamide. ○, PS spheres; ●, PS spheres in polyacrylamide solution: $M_W = 6.5 \times 10^4$, C_P = 1.0 mg/ml; ▽, PS spheres in polyacrylamide solution: $M_W = 1.0 \times 10^6$, C_P = 1.0 mg/ml.

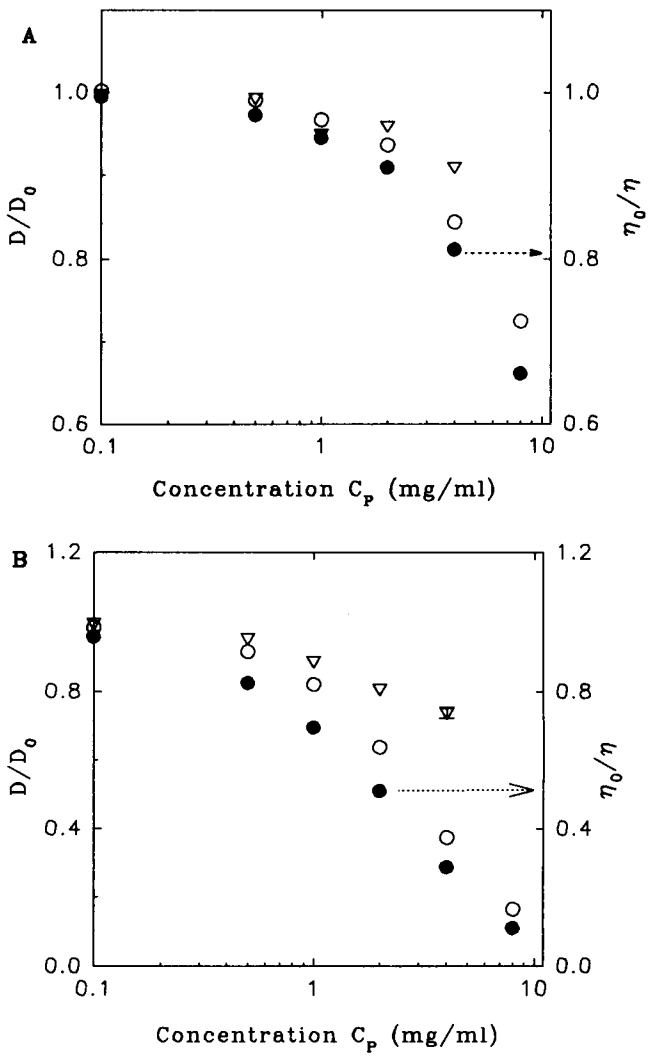

FIGURE 6 Particle diffusion coefficient versus matrix concentration for PS spheres (d = 64 nm, ○) and unilamellar lipid vesicles (d = 65 nm, ▽) in polyacrylamide solutions. (*A*) $M_w = 6.5 \times 10^4$; (*B*) $M_w = 1.0 \times 10^6$. A typical error bar (based on 9 repeated measurements) in (*B*) shows the uncertainty of the D/D_0 measurement. The inverse of the normalized viscosity, η_0/η, where η_0 is the viscosity of water (solvent) and η is the polymer solution viscosity, is also shown (●).

and unilamellar FPLC vesicles shown in Fig. 7 *B*, we also include the data for larger PS spheres (107 nm in diameter) and multilamellar extrusion vesicles in Fig. 7 *A*. Since particle size was unchanged upon the addition of the polymer, SE behavior would correspond to a constant value of unity for this ratio, $D\eta/(D_0\eta_0)$. It is quite clear that within experimental error SE diffusion behavior is well satisfied for the large PS spheres and large multilamellar vesicles diffusing in the low molecular weight PA solution (Fig. 7 *A*). For the higher molecular weight PS solution there appear to be negative deviations. In the case of the large PS spheres this negative deviation is independent of the concentration, while for the large multilamellar vesicles it is only seen at the high PA concentrations. The origin of this negative deviation is unclear. Negative deviations from the SE relation could arise from chain adsorption and/or sphere aggregation (Cooper et al., 1991; Gorti and Ware, 1985; Lin and Phillies, 1982, 1984; Ullmann and Phillies, 1983), since that would make the spheres bigger, thus diffuse slower. The magnitude of the negative deviation shown in Fig. 7 *A* is too small to arise from particle aggregation. It most likely reflects some attractive interactions between the high molecular weight PA polymer and the particle. Since TEM measurements do not show any significant adsorption or aggregation effects, we conclude that the changes in the size due to adsorption or interaction are below the resolution of TEM images.

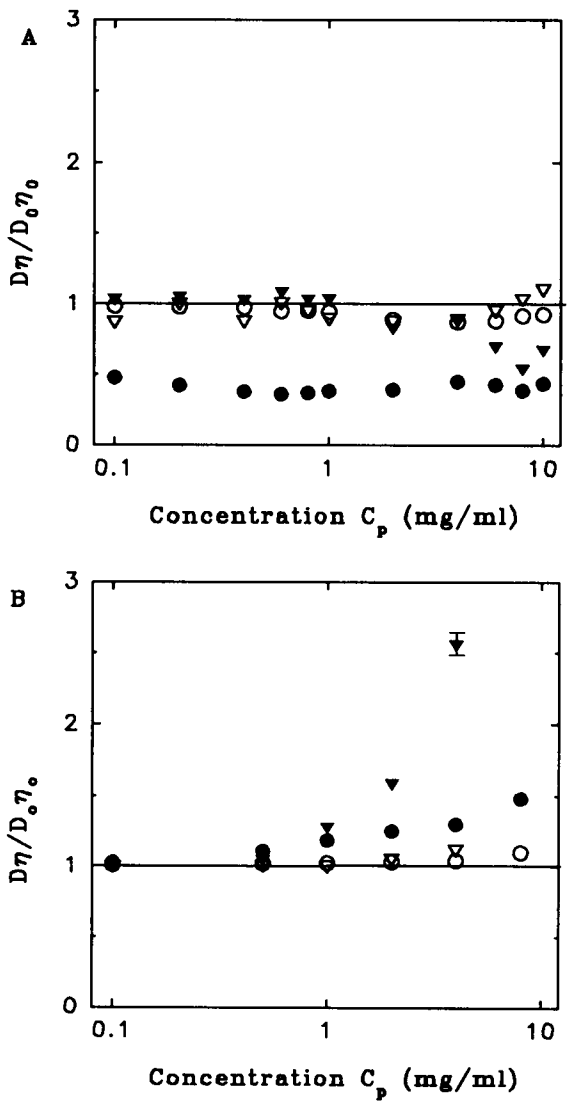

FIGURE 7 Particle diffusion behavior in relation to the Stokes-Einstein (SE) relation. The data are plotted as $D\eta/(D_0\eta_0)$, and the solid line corresponds to the SE prediction of 1 for this ratio. (*A*) Large particles (d = 105 nm multilamellar extrusion vesicles, and d = 107 nm PS spheres) in polyacrylamide solutions. ○, PS spheres in polyacrylamide solution, $M_W = 6.5 \times 10^4$; ●, PS spheres in polyacrylamide solution, $M_W = 1.0 \times 10^6$; ▽, vesicles in polyacrylamide solution, $M_W = 6.5 \times 10^4$; ▼, vesicles in polyacrylamide solution, $M_W = 1.0 \times 10^6$. (*B*) Small particles (d = 65 nm unilamellar FPLC vesicles, and d = 64 nm PS spheres) in polyacrylamide solutions. The symbols are the same as in (*A*). A typical error bar in (*B*) shows the uncertainty of the measurements.

As shown in Fig. 7 *B*, both PS spheres (d = 64 nm) and unilamellar FPLC vesicles diffuse according to the SE relation in the low molecular weight PA solution at low concentrations. In contrast, for the higher molecular weight polymer solution, the unilamellar vesicles exhibit a strong positive deviation, particularly at higher polymer concentrations, reaching $D\eta/(D_0\eta_0) = 2.6$ at $C_P = 4.0$ mg/ml (the highest concentration investigated). In this same concentration regime, the PS spheres of the same size (d = 64 nm) exhibit a much smaller positive deviation ($D\eta/(D_0\eta_0) \leq 1.5$, $D\eta/(D_0\eta_0) = 1.3$ at $C_P = 4.0$ mg/ml). Throughout the concentration range examined, the unilamellar vesicles have a more profound degree of positive deviation from the SE relation than the PS spheres, and this difference is magnified as the polymer concentration increases. In other words, the microviscosity felt by the PS spheres is only slightly smaller than the bulk viscosity, while the microviscosity felt by the unilamellar vesicles is significantly smaller than the bulk macroviscosity of the polymer solution. The difference between the micro and macroviscosity for the unilamellar vesicles increases sharply as the polymer concentration increases. Even though the bulk viscosity of the polymer solution (measured by Cannon Ubbelohde viscometer) may not precisely reflect the true value of the solution due to factors such as sticking of the polymer to glass and shear forces present, the difference between the diffusion behaviors of the small unilamellar vesicles and the PS spheres could not arise from the uncertainty of the viscosity measurement, since these two types of particles were diffusing in identical environments (same polymer solution) and the same viscosity values were used to calculate the particles' diffusivities.

The significant positive deviation from the SE relation seen with the unilamellar vesicles cannot arise from an increase in the size of the particle due to possible aggregation and/or adsorption. As pointed out by Won et al. (1994), positive deviations are observed in the vicinity of c^*, the cross-over concentration between the dilute and semi-dilute regimes. The correlation length of the polymer matrix ξ exhibits a maximum at $C_P \approx c^*$, becoming approximately

equal to the radius of gyration of the polymer. Since the layer of fluid within a distance ξ of the particle's surface will, in general, differ from the bulk solution, the particle will not sense the macroscopic solution viscosity, particularly in the vicinity of c^*. Instead, the particle encounters a reduced effective viscosity, the microviscosity. Our results can be reconciled with this picture. Since for a $M_w = 1.0 \times 10^6$ macromolecule, the overlap concentration, c^*, is $\sim$1 mg/ml, it is clear that the deviation from SE prediction for PS spheres and vesicles occurs when the matrix molecules began to overlap and entangle. For the low molecular weight polymer, the concentration regime explored was well below c^*; thus, no significant deviations were observed.

The question arises, why is the deviation so strong for the unilamellar vesicles compared to either the PS spheres or the multilamellar vesicles? Since the correlation length of the polymer should be independent of the tracer particle, we suggest that the different diffusion behaviors between the PS spheres and unilamellar vesicles are caused by their structural difference. The PS spheres are known to be hard, rigid spheres, with structure and shape remaining unchanged. On the other hand, the unilamellar vesicles have a different structure, with the lipid bilayer forming a shell that is filled on the inside with water. Such a configuration is susceptible to the surroundings, as suggested by recent studies showing that bilayers bent over when forces such as atomic force or osmotic pressure were applied to the vesicle surface, thus changing the shape of the vesicle (Hui et al., 1995; Mathivet et al., 1996; Schwartz et al., 1993; Seddon, 1990; Zasadzinski et al., 1994). Therefore, it is reasonable to assume that the vesicle's shape changes as it encounters an obstacle on its path. This ability to change its shape accounts for the vesicle's different diffusion behavior from that of a hard sphere, as demonstrated in the experimental results presented above. The effective microviscosity felt by the unilamellar vesicles is *smaller* than that felt by the PS spheres.

No positive deviation was seen for the large extrusion vesicles. This may be related to the fact that the large extrusion vesicles were a 50/50 mixture of uni and multilamellar vesicles. The multilamellar vesicles' ability to change their shape is greatly reduced due to the increase in the total thickness of their lipid layer; the thicker the layers, the stiffer are the vesicles and the closer is their diffusion to that of the hard PS spheres. In an attempt to alter the stiffness of the lipid layer, we prepared large extrusion vesicles with different cholesterol contents from cholesterol/phosphatidylcholine = 0 to 1.3:1. However, no noticeable difference was seen in the diffusion behaviors. We suspect that the stiffening effect caused by the multilamellar morphology was too big to be compensated by relatively minor changes in lipid content.

That a particle's diffusion behavior depends on its flexibility brings a whole new aspect to the field of tracer diffusion, in which much emphasis has been focused on either the concentration or the architecture of the matrix. In addition, it implies that the presence of high molecular weight macromolecules has little effect on the diffusion behavior of flexible unilamellar vesicles. This conclusion is proven to be of essential importance in the study of mucin-induced vesicle aggregation and fusion (Afdhal et al., 1995; Cao, 1997).

CONCLUSION

We have used dynamic light scattering to follow the tracer diffusion of rigid PS spheres of two different sizes (d = 64 nm and 107 nm), and two types of lipid vesicles (FPLC vesicles, unilamellar, d = 65 nm; and large extrusion vesicles, 50/50 mixture of uni and multilamellar, d = 105 nm), in aqueous solutions of PA ($M_w = 6.5 \times 10^4$ and $M_w = 1.0 \times 10^6$). Over the range of the matrix concentration examined (C_p = 0.1–10 mg/ml), the diffusivities of the PS spheres and the large extrusion vesicles exhibited mainly the Stokes-Einstein (SE) relation in low molecular weight PA solutions. Slight negative deviation was seen in high molecular weight PA solution for large particles (105 nm). However, the diffusivity of the unilamellar FPLC vesicles did not follow the increase of the solution's viscosity caused by the presence of the matrix molecules. Instead, the unilamellar vesicles exhibit a significant positive deviation from the SE behavior. This difference is attributed to the unilamellar vesicle's ability to change its shape to pass through the meshes and channels formed by the chain overlapping and entanglement of the macromolecules. In effect, the unilamellar FPLC vesicles felt a viscosity closer to that of the solvent (water), than to that of the polymer solution. A quantitative explanation for this deviation from the SE relation is not yet available, but it is probably correlated with the stiffness of the vesicle's lipid layer, the matrix concentration, and molecular weight. In conclusion, we note that the microviscosity of a polymer solution detected by a tracer diffusion measurement depends not only on the correlation length of the polymer solution and the size of the tracer particle, but also on the flexibility of the probe particle.

This work was supported by National Institutes of Health Grants DK45936 and DK47628 (to N.A. and E.M.). R.B. acknowledges the support of the National Science Foundation.

REFERENCES

Afdhal, N. H., N. Niu, D. Nunes, R. Bansil, X. Cao, D. Gantz, D. M. Small, and G. D. Offner. 1995. Mucin-vesicle interactions in model bile: evidence for vesicle aggregation and fusion before cholesterol crystal formation. *Hepatology.* 22:856–865.

Bartlett, G. R. 1959. Phosphorus assay in column chromatography. *J. Biol. Chem.* 234:466–468.

Berne, B. J., and R. Pecora. 1976. Dynamic Light Scattering. John Wiley & Sons, Inc., New York.

Brown, W., and R. Rymden. 1988. Comparison of the translational diffusion of large spheres and the high molecular weight coils in polymer solutions. *Macromolecules.* 21:840–846.

Brown, W., and P. Zhou. 1989. Dynamic behavior in ternary polymer solutions. Polybutylene in chloroform studied using dynamic light scattering and pulsed field gradient NMR. *Macromolecules*. 22:4031–4039.

Brown, W., and P. Zhou. 1990. Self-diffusion: an experimental demonstration of the non-applicability of the reptation model to semidilute solutions. *Polymer*. 31:772–777.

Cao, X. 1997. Aggregation and gelation of mucin and its interactions with lipid vesicles. Ph.D. thesis. Boston University.

Cohen, D. E., and M. C. Carey. 1990. Rapid (1 hour) high performance gel filtration chromatography resolves coexisting simple micelles, mixed micelles and vesicles in bile. *J. Lipid Res.* 31:2103–2112.

Cooper, E. C., P. Johnson, and A. M. Donald. 1991. Probe diffusion in polymer solutions in the dilute/semi-dilute crossover regime. 1. Poly(ethylene oxide). *Polymer*. 32:2815–2822.

Forte, T. M., and R. W. Nordhausen. 1986. Electron microscopy of negative stained lipoproteins. *Methods Enzymol.* 128:442–456.

Gorti, S., and B. R. Ware. 1985. Probe diffusion in an aqueous polyelectrolyte solution. *J. Chem. Phys.* 83:6449–6456.

Hui, S. W., R. Viswanathan, J. A. Zasadzinski, and J. N. Israelachvili. 1995. The structure and stability of phospholipid bilayers by atomic force microscopy. *Biophys. J.* 68:171–178.

Lin, T-H., and G. D. J. Phillies. 1982. Translational diffusion coefficient of a macromoleculate probe species in salt-free poly(acrylic acid)-water. *J. Phys. Chem.* 86:4073–4077.

Lin, T-H., and G. D. J. Phillies. 1984. Probe diffusion in poly(acrylic acid)-water. Effect of probe size. *Macromolecules*. 17:1686–1691.

MacDonald, R. C., R. I. MacDonald, B. Menco, K. Takeshita, N. K. Subbarao, and L. Hu. 1991. Small-volume extrusion apparatus for preparation of large, unilamellar vesicles. *Biochim. Biophys. Acta*. 1061: 297–303.

MacDonald, R. I., N. Oku, and R. C. MacDonald. 1983. Liposome formation, re-visited. *In* The Liposome Letters, A. D. Bangham, editor. Academic Press, London, 63–72.

Madonia, F., P. L. San Biagio, M. U. Palma, G. Schiliro, S. Musumeci, and G. Russo. 1983. Photon scattering as a probe of microviscosity and channel size in gels such as sickle hemoglobin. *Nature*. 302:412–415.

Mathivet, L., S. Cribier, and P. Devaux. 1996. Shape change and physical properties of giant phospholipid vesicles prepared in the presence of an AC electric field. *Biophys. J.* 70:1112–1121.

Mayer, L. D., M. J. Hope, P. R. Cullis, and A. S. Janoff. 1985. Solute distributions and trapping efficiencies observed in freeze-thawed multilamellar vesicles. *Biochim. Biophys. Acta*. 817:193–196.

National Research Council. 1988. Frontiers in Chemical Engineering. National Academy Press, Washington, DC.

Nehme, O. A., P. Johnson, and A. M. Donald. 1989. Probe diffusion in poly-L-lysine solution. *Macromolecules*. 22:4326–4333.

Newman, J., N. Mroczka, and K. L. Schick. 1989. Dynamic light scattering measurements of the diffusion of probes in filamentous actin solutions. *Biopolymers*. 28:655–666.

Newman, J., and K. L. Schick. 1989. Probe diffusion in cross-linked actin gels. *Biopolymers*. 28:1969–1980.

Onyenemezu, C. N., D. Gold, M. Roman, and W. G. Miller. 1993. Diffusion of polystyrene latex spheres in linear polystyrene non-aqueous solutions. *Macromolecules*. 26:3833–3837.

Phillies, G. D. J. 1988. Quantitative prediction of α in the scaling law for self-diffusion. *Macromolecules*. 21:3101–3106.

Phillies, G. D. J. 1989. The hydrodynamic scaling model for polymer self-diffusion. *J. Phys. Chem.* 93:5029–5039.

Phillies, G. D. J. 1990. Chain architecture in the hydrodynamic scaling picture for polymer solutions. *Macromolecules*. 21:3101–3106.

Phillies, G. D. J., C. Malone, G. S. Ullmann, J. Rollings, and L.-P. Yu. 1987. Probe diffusion in solutions of long-chain polyelectrolytes. *Macromolecules*. 20:2280–2289.

Phillies, G. D. J., and P. Peczak. 1988. The ubiquity of stretched-exponential forms in polymer dynamics. *Macromolecules*. 21:214–220.

Pope, J. L. 1967. Crystallization of sodium taurocholate. *J. Lipid Res.* 8:146–147.

Provencher, S. W., J. Hendrix, L. De Maeyer, and N. Paulussen. 1978. Direct determination of molecular weight distributions of polystyrene in cyclohexane with photon correlation spectroscopy. *J. Chem. Phys.* 69: 4273–4276.

Reina, J. C., R. Bansil, and C. Konak. 1990. Dynamics of probe particles in polymer solutions and gels. *Polymer*. 31:1038–1044.

Rudell, L. L., and M. D. Morris. 1973. Determination of cholesterol using O-phthaldehyde. *J. Lipid Res.* 14:364–366.

San Biagio, P. L., J. Newman, and K. L. Schick. 1991. Dynamic light scattering from spatially inhomogeneous cross-linked actin gels. *Macromolecules*. 24:6794–6796.

Schwartz, D. K., J. Garnaes, R. Viswanathan, S. Chiruvolu, and J. A. Zasadzinski. 1993. Quantitative lattice measurement of thin Langmuir-Blodgett films by atomic force microscopy. *Phys. Rev. E*. 47:452–460.

Seddon, J. M. 1990. Structure of the inverted hexagonal (H_{II}) phase, and non-lamellar phase transitions of lipids. *Biochim. Biophys. Acta*. 1031: 1–69.

Smith, B. F. J. 1987. Human gallbladder mucin binds biliary lipids and promotes cholesterol crystal nucleation in model bile. *J. Lipid Res.* 28:1088–1097.

Somjen, G. J., Y. Marikovsky, P. Lelkes, and T. Gilat. 1986. Cholesterol-phospholipid vesicles in human bile: an ultrastructural study. *Biochim. Biophys. Acta*. 879:14–21.

Tracy, M. A., and R. Pecora. 1992. Synthesis, characterization, and dynamics of a rod/sphere composite liquid. *Macromolecules*. 25:337–349.

Turley, S. D., and J. M. Dietschy. 1978. Re-evaluation of the 3α-hydroxysteroid dehydrogenase assay for total bile acids in bile. *J. Lipid Res.* 19:924–928.

Ullmann, G., and G. D. J. Phillies. 1983. Implications of the failure of the Stokes-Einstein equation for measurements with QELSS of polymer adsorption by small particles. *Macromolecules*. 16:1947–1949.

Won, J., C. Onyenemezu, W. G. Miller, and T. P. Lodge. 1994. Diffusion of spheres in entangled polymer solutions: a return to Stokes-Einstein behavior. *Macromolecules*. 27:7389–7396.

Zasadzinski, J. A., R. Viswanathan, L. Madsen, J. Garnaes, and D. K. Schwartz. 1994. Langmuir-Blodgett films. *Science*. 263:1726–1733.

Zhou, P., and W. Brown. 1989. Translational diffusion of large silica spheres in semidilute polyisobutylene solutions. *Macromolecules*. 22: 890–896.